RESEARCH PAPER

WILEY | Journal of Biogeography

Past vegetation dynamics in the Yellowstone region highlight the vulnerability of mountain systems to climate change

Virginia Iglesias[1] | Cathy Whitlock[1,2] | Teresa R. Krause[2] | Richard G. Baker[3]

[1]Montana Institute on Ecosystems, Montana State University, Bozeman, MT

[2]Department of Earth Sciences, Montana State University, Bozeman, MT

[3]Department of Earth and Environmental Sciences, University of Iowa, Iowa City, IA

Correspondence
Virginia Iglesias, Montana Institute on Ecosystems, Montana State University, Bozeman MT, 59715.
Email: virginia.iglesias@colorado.edu

Present address
Virginia Iglesias, Earth Lab, University of Colorado, Boulder, CO.

Abstract

Aim: Reconstruct the long-term ecosystem dynamics of the region across an elevational gradient as they relate to climate and local controls. In particular, we (1) describe the dominant conifers' history; (2) assess changes in vegetation composition and distribution; and (3) note periods of abrupt change versus stability as means of better understanding vegetation responses to environmental variability.

Location: Greater Yellowstone Ecosystem (GYE; USA).

Time period: 16.5 ka BP-present.

Major taxa studied: *Juniperus, Picea, Abies, Pinus, Pseudotsuga.*

Methods: The vegetation reconstruction was developed from 15 pollen records. Results were interpreted based on modern pollen–vegetation relationships estimated from a suite of regression-based approaches.

Results: Calibrated pollen data suggest that late-glacial vegetation, dominated by shrubs and *Juniperus*, lacks a modern counterpart in the area. *Picea, Abies* and *Pinus* expanded at 16 ka BP in association with postglacial warming and co-occurred in mixed-conifer parkland/forest after 12 ka BP. This association along with *Pinus contorta* forest, which was present after 9 ka BP, has persisted with little change at middle and high elevations to the present day. This stability contrasts with the dynamic history of plant communities at low elevations, where shifts between parkland, steppe and forest over the last 8,000 years were likely driven by variations in effective moisture and fire.

Main conclusions: The postglacial vegetation history of the GYE highlights the dynamic nature of mountain ecosystems and informs on their vulnerability to future climate change: (1) most of the conifers have been present in the area for >12,000 years and survived climate change by adjusting their elevational ranges; (2) some plant associations have exhibited stability over millennia as a result of nonclimatic controls; and (3) present-day forest cover is elevationally more compressed than at any time in history, probably due to the legacy of the Medieval Climate Anomaly and the Little Ice Age.

KEYWORDS
climate change, conifers, pollen–vegetation calibration, postglacial, stability, Yellowstone

1 | INTRODUCTION

The Greater Yellowstone Ecosystem (GYE), an 80,000 km^2 mountainous region in western North America, is one of the last remaining, nearly intact ecosystems in the mid-latitudes. The origins of the GYE, as we know it today, trace back 20,000 years ago, when the region was covered by a large glacial complex (Licciardi & Pierce, 2008). Ice recession and warming temperatures after 17 ka BP (ka BP = kilo annum before present) created vast new areas for biotic colonization and subsequent ecosystem development (Krause & Whitlock, 2017). As in most regions, our understanding of the ecological history of the GYE comes from pollen records obtained from sediment cores of natural lakes and wetlands that formed during deglaciation, and this history has been discussed in a series of papers dating back to the mid-1970s (Baker, 1976; Huerta, Whitlock & Yale, 2009; Iglesias, Krause, & Whitlock, 2015; Krause & Whitlock, 2013, 2017; Krause, Lu, Whitlock, Fritz, & Pierce, 2015; Millspaugh, Whitlock, & Bartlein, 2000, 2004; Mumma, Whitlock, & Pierce, 2012; Waddington & Wright, 1974; Whitlock, 1993; Whitlock & Bartlein, 1993; Whitlock et al., 2012). Most of these studies are site-specific, and there has been little effort at broader interpretations across the GYE. For this reason, our understanding of the long-term vegetation dynamics across elevation and geography is rather poor, although not atypical of mountainous regions in general.

The relationship between modern pollen and present-day vegetation is the primary tool for reconstructing vegetation and species history based on fossil pollen data. At some sites, the presence of plant macrofossils in the sediment cores can add precision to these interpretations, and analysis of particulate charcoal provides complementary information on past fire activity (Whitlock & Larsen, 2001). Quantifying pollen–vegetation relationships in mountainous regions, like the GYE, has proven to be particularly challenging for two reasons. First, mountain vegetation types tend to be arrayed by elevation (i.e. zonal), and upslope transport of pollen from plants growing at low and middle elevations often obscures the distinctiveness of pollen assemblages at higher elevations (Markgraf, Webb, Anderson, & Anderson, 2002; Minckley & Whitlock, 2000). Second, in temperate regions, mountains support taxa that are large pollen producers (e.g. *Pinus*, *Fagus*, *Nothofagus*), and these taxa dominate the pollen rain far beyond the species distribution (Cañellas-Boltà, Rull, Vigo, & Mercadé, 2009; Iglesias, Quintana, Nanavati, & Whitlock, 2016; Minckley & Whitlock, 2000). As a result, modern pollen assemblages from different elevations are often qualitatively similar, and their interpretation is not straightforward.

This study seeks to improve our understanding of the elevational patterns of vegetation change in the GYE based on modern and fossil pollen data. Our approach is to estimate the relationship between present-day pollen rain and vegetation and then apply the empirical relationships to a fossil pollen dataset that includes records from low, middle and high elevations and spans the last 16,500 years. By examining temporal and spatial changes in pollen assemblages, our objectives are as follows: (1) describe the history of the region's dominant conifers as it relates to large-scale climatic and nonclimatic controls; (2) reconstruct the vegetation history since deglaciation across an elevational gradient and identify periods and locations when past vegetation was fundamentally different from present (i.e. no-analogue communities, sensu Williams & Jackson, 2007) and (3) note periods of abrupt ecological change as well as stability in the past as means of better understanding long-term ecosystem dynamics. This calibrated, multisite reconstruction highlights the resilience of GYE vegetation to past environment change, and the findings have relevance for assessing ecosystem vulnerability in the future.

1.1 | Study area

The GYE is located within the northern Rocky Mountains and encompasses areas of north-western Wyoming, south-western Montana and eastern Idaho, USA. It features a central rhyolitic plateau region formed as part of the Yellowstone Caldera "hot spot," and this relatively flat region is surrounded by mostly north–south trending mountain ranges with peaks that exceed 4,000 m in elevation.

Temperatures in the GYE range from −13°C in January to 26°C in July and August. Most of the precipitation is received from Pacific storm systems in winter and spring, whereas summer precipitation is geographically variable. Monsoonal circulation from the Gulf of Mexico and the subtropical Pacific Ocean increases the probability of summer convective storms, especially in the eastern and southern regions. Conversely, the north-eastern Pacific subtropical high-pressure system tends to suppress precipitation in the western region, where summer conditions are relatively dry (Whitlock & Bartlein, 1993).

The present-day vegetation of the GYE is generally arrayed by elevation as a result of colder conditions and a shorter growing season at higher elevations and decreased moisture availability at low elevations. Local conditions arising from aspect and substrate, which is governed by underlying geology, disrupt the altitudinal zonation in some locations. Overall, at elevations below c. 1,600 m in the GYE, a Steppe Zone is dominated by *Artemisia* (primarily *A. tridentata*), but other shrubs (e.g. *Purshia tridentata*, *Sarcobatus vermiculatus*, *Ericameria nauseosa*) and perennial grasses (e.g. *Festuca idahoensis*, *Poa* spp, *Pseudoroegneria spicata*) are also present. Woodland and shrubland (Steppe/parkland Zone, 1,600–1,900 m elev) comprise the lower tree line, and tree cover becomes denser with increasing elevation and higher moisture availability. Conifer dominants in lower parkland (i.e. *Pseudotsuga* Parkland Zone, 1,900–2,000 m elev in northern GYE) include *Pseudotsuga menziesii*, *Pinus flexilis* and *Juniperus scopulorum*. At higher elevations, the *Pinus contorta* Forest Zone (2,000–2,400 m elev) is strongly governed by soil type and disturbance regime, and closed *P. contorta* Forest prevails on nutrient-poor well-drained rhyolite substrates of the Central Plateau region of Yellowstone National Park, as well as on recently burned landscapes. At higher elevations (2,400–2,800 m elev) and on more fertile soils the Mixed-conifer Forest Zone supports *Picea engelmannii*, *Abies lasiocarpa*, *Pinus*

contorta and *Pinus albicaulis*, and site composition is strongly driven by time since disturbance. Dominated by the same conifers but at lower densities, the Mixed-conifer Parkland Zone occurs above 2,800 m elev, although *P. albicaulis* occasionally forms pure stands in this zone. The Tundra Zone (>2,900 m elev) supports a diverse array of shrubs and herbs. Cross-elevational plant communities include aspen (*Populus tremuloides*) forest, which grows from the foothills to the subalpine region in areas of deep moist soil, and riparian communities of *Salix* spp., *Betula occidentalis*, *Alnus incana*, *Populus* spp., *Spiraea douglasii* and *Acer glabrum*.

2 | MATERIALS AND METHODS

2.1 | Modern pollen calibration

We compiled modern pollen samples from high-elevation tundra to low-elevation steppe to calibrate pollen–vegetation relationships in the GYE. In order to ensure replicable results, we calculated an "optimal pollen sum." This value was determined through rarefaction analysis and defined as the point where the first derivative of the richness of the sample as a function of the number of grains identified tended to zero (i.e. smaller counts would result in information loss and larger ones would not increase significantly the probability of detecting new pollen types; Sanders, 1968). Independent of the size of the lake where the samples were collected, rarefaction analysis suggests that pollen sums larger than 365 grains assure the presence of at least 16 pollen types (the median palynological richness of the dataset) in 75% of the samples. Only samples whose pollen sum exceeded that value and that distinguished between *Pinus* pollen types were included in the study.

The resulting dataset consists of 84 surface samples and core tops collected from small-, medium- and large-sized lakes (<80 m², 80–70,000 m² and >70,000 m² respectively) located from the Yellowstone River valley in the northwest to the Wind River Range in the southeast (Table S1 in Appendix S1, Figure 1). A vegetation zone was assigned to each sample based on site elevation and descriptions from the original study (Table S1 in Appendix S1; Figure 2). It is noteworthy that some samples were collected over 50 years ago, and the original assignment does not always describe present-day vegetation at the site, especially in locations where forests have been destroyed by recent wildfires or insect infestations.

Pollen percentages were calculated for each sample based on the sum of all terrestrial types. The source of *Pinus* subgenus *Strobus*-type pollen was attributed to *P. albicaulis* and/or *P. flexilis*, and *Pinus* subgenus *Pinus*-type pollen comes from either *P. contorta* or
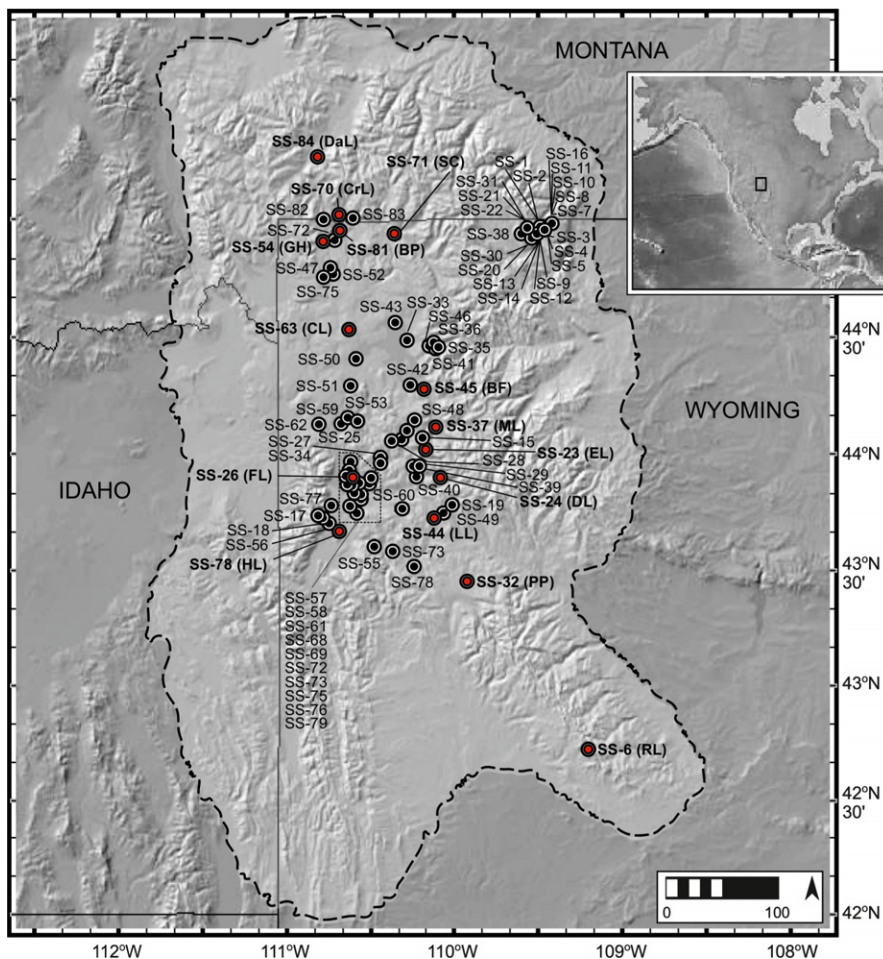

FIGURE 1 Location of the sites employed in the modern pollen–vegetation calibration (all circles; Table S1 in Appendix S1) and in the reconstruction of the postglacial vegetation history (in red; RL: Rapid Lake; ML: Mariposa Lake; PP: Park Pond; EL: Emerald Lake; DL: Divide Lake; FL: Fallback Lake; CL: Cygnet Lake; LL: Lily Lake; BF: Buckbean Fen; GH: Gardiner's Hole; BP: Blacktail Pond; SC: Slough Creek; CrL, Crevice Lake; DaL: Dailey Lake; Table S1 in Appendix S2). The dashed line shows the boundary of Greater Yellowstone Ecosystem [Colour figure can be viewed at wileyonlinelibrary.com]
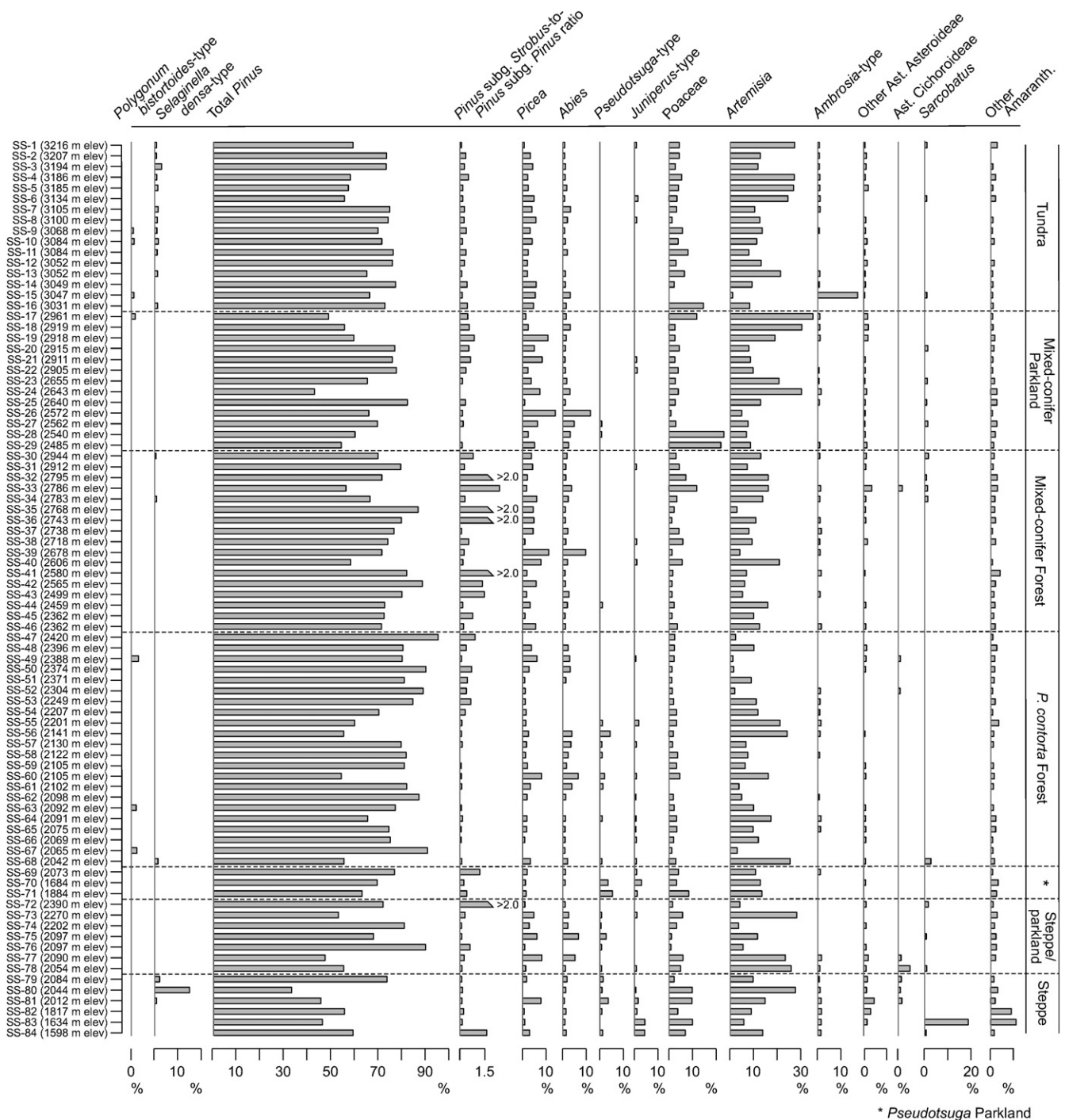
FIGURE 2 Modern pollen percentage data for selected taxa plotted according to present-day vegetation zones (Ast. = Asteraceae; Amaranth. = Amaranthaceae). The geographical location of samples is shown on Figure 1

* *Pseudotsuga* Parkland

P. ponderosa. Because *P. ponderosa* is currently absent in most of the GYE and there is no plant macrofossil evidence of its presence since the previous interglaciation (Baker & Richmond, 1978), we attribute this pollen type largely to *P. contorta*. *Picea* pollen may have come from *P. engelmannii*, possibly *P. glauca* in the late-glacial period, and *P. pungens*, which is a minor species in the southern GYE. *Pseudotsuga* and *Larix* have indistinguishable pollen, but only *Pseudotsuga menziesii* grows in the region. *Juniperus*-type

pollen is attributed to *J. scopulorum*, *J. communis* and *J. horizontalis*, and their collective distribution spans all elevations. At some sites, plant macrofossils (e.g. needles, seeds, bracts) in the sediment cores help confirm the pollen assignments (Brunelle, Whitlock, Bartlein, & Kipfmuller, 2005).

Estimation of modern pollen–vegetation relationships was performed with classification trees and optimal thresholds of dissimilarity applied to pollen percentage data. Classification trees are based

on the recursive partitioning of the multidimensional space defined by the predictor variables (i.e. modern pollen data from all sites) into response variables (i.e. vegetation; (Breiman, Friedman, Stone, & Olshen, 1984)). This methodology, which is free of distributional assumptions, resulted in two binary decision keys. The first key allowed the estimation of the local abundance of conifers in the landscape. To this end, we calculated thresholds for pollen percentages of *Pinus* subgenus *Strobus*, *Pinus* subgenus *Pinus*, *Picea*, *Abies*, *Pseudotsuga*-type and *Juniperus*-type based on whether the taxon was "abundant" or "rare/absent" at each site. The conifers were considered "abundant" when they accounted for more than about 20% of the local tree cover and "rare/absent" when they were present at very low densities at most.

The second classification tree considered all possible splits for all terrestrial pollen types and separated the pollen samples into three cover classes. Cover classes constitute a qualitative representation of the proportion of trees relative to open ground, grasses and shrubs on the landscape (i.e. Forest, Parkland and Steppe/Tundra). Information on the local abundance of conifers and cover-class assignment were based on published site descriptions (Table S1 in Appendix S1). We used 10-fold cross-validation and "pruned" all classification trees to avoid overfitting and allow generalization to independent pollen datasets (Ripley, 1996). In all cases, the effect of lake size (Table S1 in Appendix S1) on classification was assessed. Misclassification error rates (MER) [1] are reported to allow evaluation of the overall performance of the trees.

$$MER = (FP + FN)/T \qquad (1)$$

with FP: total number of false positives resulting from the classification; FN: total number of false negatives resulting from the classification and T: total number of samples.

Finally, optimal thresholds of dissimilarity were employed to calculate the probability of pollen samples belonging to each vegetation zone. In particular, we computed a dissimilarity matrix based on the squared-chord distances (SCDs) between all pairs of modern pollen samples and compared the within- and between-zones SCDs. Following Overpeck, Webb, and Prentice (1985), we defined thresholds of dissimilarity as the largest SCD between two pollen samples that originated from the same vegetation zone. A threshold of zero would imply that only palynologically identical samples belong to the same vegetation zone. However, due to both natural and analytical variability, dissimilarity values larger than zero are expected between pollen samples from the same plant community. Thresholds of dissimilarity were larger than zero to allow for variability but small enough to ensure the discrimination of pollen samples from different vegetation types. To optimize this discrimination, we generated the expected distribution of SCDs with 1,000 Monte Carlo simulations. Cutoffs that were unlikely to have occurred by chance (i.e. $p = .01$, .025 and .05) were identified as optimal thresholds of dissimilarity among different vegetation zones (Sawada, Viau, Vettoretti, Peltier, & Gajewski, 2004).

2.2 | Species and vegetation history reconstructions

The conifer and vegetation history of the GYE was inferred from 15 published pollen records extending from present-day steppe to alpine tundra (1,684 to 3,134 m elev; Table S1 in Appendix S2). Percentages were calculated on the same terrestrial pollen sum as the modern dataset. We reconstructed population dynamics of the six dominant conifer taxa (i.e. *Juniperus*, *Picea*, *Abies*, *Pinus albicaulis* and/or *P. flexilis*, *Pinus contorta* and *Pseudotsuga*) by linearly interpolating site-specific pollen percentages onto a grid defined by time and elevation (i.e. pollen isolines = lines of equal pollen abundance; Akima, 1978). The modern abundance thresholds were then applied to the interpolated fossil data to determine where and when taxa were rare/absent or abundant and to estimate the errors in the assignment.

The reconstruction of past vegetation was performed through space-for-time substitutions (i.e. through identification of similar communities in the present-day landscape). Specifically, we calculated the square-chord distance between samples in each fossil record (Table S1 in Appendix S2) and the suite of modern samples compiled for this study (Table S1 in Appendix S1). Application of optimal thresholds of dissimilarity allowed us to identify the most likely modern analogue for the fossil pollen assemblages. Fossil samples were assigned to a modern vegetation zone when the SCD between the fossil sample and a modern one was smaller than expected by chance ($p < .05$). No-analogue communities were identified when SCD values exceeded the optimal threshold of dissimilarity. It is noteworthy that analogue detection is dependent on the training dataset (in our case, pollen samples from the GYE). Therefore, "no-analogue vegetation" in this study refers to plant communities with no modern counterpart in the GYE, and we recognize that modern pollen samples from elsewhere in the western U.S. may have provided a suitable match for these assemblages.

In order to assess variability in vegetation composition, we calculated SCDs between fossil samples and the youngest sample of each record. The site-specific results were interpolated onto a grid defined by time and elevation, and abrupt changes in vegetation were identified through sequential Lepage testing (3 sample-sequences; 0.05 alpha-level). Prior to interpolation, the SCD time series were subsampled at the median resolution of all series (i.e. 354 years) to avoid overrepresentation of records with a larger number of samples. All analyses and figures were performed with R programming language (R Core Team, 2016), packages "akima" version 0.6-2 (Akima & Gebhardt, 2016), "ggplot2" (Wickham, 2016), "MAT-TOOLS" version 1.1 (Sawada, 2012), "rioja" version 0.9-15 (Juggins, 2017), "vioplot" version 0.2 (Adler, 2005), "tree" version 1.0–37 (Ripley, 2016) and corresponding dependencies.

3 | RESULTS

Visual inspection of modern pollen samples from the GYE indicates that the pollen rain in all vegetation zones is dominated by total *Pinus* and, to a lesser extent, *Artemisia* (Figure 2). Samples from the

TABLE 1 Local-abundance thresholds for conifers as predicted by cross-validated classification trees and their respective misclassification error rates (MER). Only MERs lower than 26% are reported

Pinus albicaulis/Pinus flexilis

(1a) *Pinus Strobus*-to-*Pinus Pinus* ratio < 0.4 _____ **Rare/absent** (MER=21%

(1b) *Pinus Strobus*-to-*Pinus Pinus* ratio > 0.4 _____ **Abundant** (MER=18%)

Pinus contorta

(1a) Total *Pinus* < 77.2 % _____ **Rare/absent** (MER=20%)

(1b) Total *Pinus* > 77.2 % _____ (2)

    (2a) Total *Pinus* < 87.1 % _____ (3)

        (3a) *Pinus Strobus*-to-*Pinus Pinus* ratio< 0.4 ___ **Abundant** (MER=25%)

        (3b) *Pinus Strobus*-to-*Pinus Pinus* ratio > 0.4 _ **Rare/absent** (MER=17%)

    (2b) Total *Pinus* > 87.1 % _____ **Abundant** (MER=0%)

Picea spp.

(1a) *Picea* < 1.0 % _____ **Rare/absent** (MER=0%)

(1b) *Picea* > 1.0% _____ (2)

    (2a) *Picea* > 6.1% _____ **Abundant** (MER=27%)

Abies lasiocarpa

(1a) *Abies* < 0.8 % _____ **Rare/absent** (MER=21%)

(1b) *Abies* > 0.8% _____ (2)

    (2) Lake size < 80 m^2 _____ (3)

        (3a) *Abies* < 3.5 % _____ **Rare/absent** (MER=19%)

        (3b) *Abies* > 3.5 % _____ **Abundant** (MER=20%)

Pseudotsuga menziesii

(1a) *Pseudotsuga*-type < 0.2 % _____ **Rare/absent** (MER=13%)

(1b) *Pseudotsuga*-type > 0.2% _____ (2)

    (2a) *Pseudotsuga*-type > 2.5 % _____ **Abundant** (MER=20%)

Juniperus spp.

(1a) *Juniperus*-type < 1.2 % _____ **Rare/absent** (MER=23%)

Tundra Zone featured relatively low pollen percentages of open landscape taxa (e.g. *Polygonum bistortoides*-type < 1.75% and *Selaginella densa*-type <3%) and significant amounts of pollen produced by conifers growing at lower elevations (e.g. *Pinus* <78%, *Picea* <6% and *Abies* <4%). Poaceae, Asteraceae subfam. Asteroideae and Amaranthaceae pollen were present at <13%. Samples from the Mixed-conifer Parkland and Mixed-conifer Forest zones had high pollen percentages of Total *Pinus*, *Picea* and *Abies* (<87%, <14% and <12% respectively). The main difference between pollen assemblages from parkland and forest was the higher ratio of *Pinus* subgenus *Strobus* to *P.* subgenus *Pinus* in the Mixed-conifer Forest Zone (<15, as opposed to <2 in the Mixed-conifer Parkland). This difference probably reflects greater abundance of *P. albicaulis* in high-elevation forests. High total *Pinus* (up to 90%) and low ratios of *Pinus* subgenus *Strobus* to *P.* subgenus *Pinus* (<1.3) characterized the *P. contorta* Forest. Pollen of *Pseudotsuga*-type and *Juniperus*-type was almost always present in samples from the *Pseudotsuga* Parkland Zone (<8%

and <3.2% respectively). Samples from the Steppe/parkland and Steppe zones featured lower Total *Pinus* pollen percentages (mean = 56%) than other associations, and *Selaginella densa*-type and Other Amaranthaceae attained their highest abundance (<15.1 and <12% respectively).

The large degree of overlap in the palynological composition of samples confirms that discrimination of vegetation zones based solely on the most abundant pollen types is not possible in mountainous settings, such as the GYE. Despite the reduced sensitivity of most taxa, however, extreme values in the abundance of some pollen types provide insights into the plant communities that produced them. For example, *Pseudotsuga*-type was almost always present in the *Pseudotsuga* Parkland Zone, and *Selaginella densa*-type and Other Amaranthaceae attained exceptionally large values in the Steppe Zone (<15.1% and <12% respectively).

A nonunique relationship between modern pollen and vegetation arises mainly from convergence (i.e. similar pollen rain deriving from

Arboreal-to-nonarboreal pollen ratios	
(1a) Arboreal-to-nonarboreal pollen ratio > 5.9 _____ **Forest** or **Parkland** (MER=0%)	

All pollen taxa	
(1a) *Selaginella densa*-type < 0.56 % _____ (2)	
(2a) Total *Pinus* < 70% _____ **Parkland** (MER=40%)	
(2b) Total *Pinus* > 70% _____ **Forest** (MER=30%)	
(1a) *Selaginella densa*-type > 0.56 % _____ **Steppe/Tundra** (MER=20%)	

TABLE 2 Cover classes as predicted by cross-validated classification trees based on arboreal-to-nonarboreal pollen ratios or the composition of the 84 modern pollen samples. Misclassification error rates (MER) are indicated

different vegetation zones) of assemblages from the *Pseudotsuga* Parkland and Steppe/Parkland zones and from the Tundra and Steppe zones and, to a lesser extent, from divergence (i.e. different pollen spectrum from a single zone) of samples from the Mixed-conifer Forest and *Pinus contorta* Forest zones. This issue motivated the use of cross-validated classification trees to (a) estimate the probability of conifers being locally rare/absent or abundant and (b) separate pollen assemblages into cover classes.

The first binary decision key allowed us to infer the local abundance of *Pinus albicaulis/P. flexilis*, *P. contorta*, *Picea* and *Pseudotuga* based on *Pinus* subgenus *Strobus*-to-*P.* subgenus *Pinus* ratios and pollen percentages of total *Pinus*, *Picea* and *Pseudotsuga*-type respectively. The misclassification error rates for these taxa were <27% and independent of the size of the lake where the pollen sample was collected (Table 1). In the case of *Abies* and *Juniperus*-type pollen percentages, it was possible to identify rarity/absence but not abundance of the conifer. Incorporation of lake size as a predictive variable improved the ability to assess *Abies* abundance, in that samples from ponds (lakes <80 m^2) were better predictors of abundance than larger water bodies. *Juniperus*-type pollen, however, was not useful for inferring local abundance of the conifer even when waterbody size was considered.

Pollen assemblages were then separated into cover classes namely, Forest Cover, which comprised samples from the Mixed-conifer Forest and *Pinus contorta* Forest zones; Parkland Cover, which included samples from the Mixed-conifer Parkland and *Pseudotsuga* Parkland zones; and Open Cover, combining samples from the Steppe and Tundra zones. Classification was performed with two classification trees, one with the ratio of arboreal-to-nonarboreal pollen types as the only predictor, and the other one considering all pollen types as explanatory variables. Arboreal-to-nonarboreal pollen ratios from the Forest and Parkland Cover classes ranged between 0.5 and 23.7. The distribution of the ratios did not reveal a clear distinction between these two classes, but values were statistically larger than the ratios from the Open Cover class (Table 2). A critical arboreal-to-nonarboreal pollen ratio of 5.9 was identified as a threshold separating forest/parkland sites from nonforested sites, inasmuch as larger values were only observed in assemblages from the Forest and Parkland Cover classes. It is noteworthy that sample ratios smaller than 5.9 were noninformative, in that they could have come from any of the three cover classes. Therefore, although it was not possible to infer an absence of

trees on the landscape based on this method, the presence of trees could be predicted with confidence.

When all palynomorphs were included independently in the classification tree, *Selaginella densa*-type and Total *Pinus* emerged as taxa with high predictive power (Table 2). *Selaginella densa*-type values >0.56% were associated with open habitats, such as those in the Steppe/Tundra zones (MER = 20%), and lower percentages were observed in forested landscapes. Pollen samples with *Selaginella densa*-type >0.56% and Total *Pinus* <70% were characteristic of Parkland Cover class (MER = 40%), whereas Total *Pinus* >70% prevailed in assemblages from the Forest Cover class (MER = 20%).

In order to further refine the modern vegetation-pollen calibration, we estimated the similarity between all pairs of modern pollen samples with squared-chord distances (SCDs). The SCDs ranged between 0.01 and 0.5, and their frequency showed a right-skewed distribution (Figure 3). A Monte Carlo simulation (1,000 runs) indicated that SCDs of 0.02, 0.041 and 0.046 were unlikely to be obtained by random comparison of samples at a 0.01, 0.025 and 0.05 significance level, respectively. These values therefore constituted thresholds of dissimilarity with different associated uncertainties (i.e. both the sensitivity of the test and the probability of false positives decreased with lower significance levels) and allowed discrimination of all vegetation zones considered in this study.

4 | DISCUSSION

4.1 | Postglacial conifer history in the GYE

The postglacial history of the dominant conifers in the GYE was inferred from pollen abundance patterns through time and, where present, site-specific plant macrofossil data. The application of abundance thresholds (Table 1) defined the location in the space-time continuum where species were rare/absent or abundant, as well as the probability of error in the assignment (Figure 4).

The calibrated vegetation reconstruction suggests that open landscapes dominated the GYE prior to 16 ka BP (*p* > .79; Table 2). The absence or rarity of conifers at this time, however, does not rule out the possibility that small isolated populations grew near ice margins in undetected settings. These types of microrefugia seem likely given the rapid rates of conifer expansion into deglaciated areas after 16 ka BP (Krause & Whitlock, 2017).

Juniperus was probably present before 14 ka BP at elevations above 2,200 m (Figure 4). Given its broad climatic tolerances (Thompson, Anderson, & Bartlein, 1999), *J. communis* was the most likely species at the time. Pollen percentages decreased between 13 and 10 ka BP with the arrival of other conifers, indicating that populations were smaller than before ($p > .73$; Table 1). This decline is consistent with the present-day role of *J. communis* as a minor component of the forest understorey (Whitlock, 1993). Higher *Juniperus*-type percentages at 9 ka BP at low elevations (<2,200 m elev) probably record the establishment of *J. scopulorum* and/or *J. horizontalis* as a constituent of steppe and parkland vegetation.

Picea populations were relatively large below 2,400 m elev at 16 ka BP ($p > .73$; Table 1; Figure 4). Both *Picea engelmannii* and *P. glauca* were likely present, as evidenced by genetic studies that indicate the existence of hybrids in the modern GYE (Haselhorst & Buerkle, 2013). As the temperature increased and slopes stabilized after 13 ka BP (Krause & Whitlock, 2017), *Picea* expanded to higher elevations (>2,400 m elev) and became abundant above its current elevation of 2,900 m ($p > .73$; Table 1). Macrofossils at Fallback Lake, Emerald Lake, Divide Lake, Mariposa Lake and Buckbean Fen confirm local presence of the genus (Whitlock, 1993). The pollen evidence suggests large populations above 2,400 m elev between *c.* 12 and 7.5 ka BP and low *Picea* abundance below that elevation. Possibly in response to decreasing summer temperatures after 7.5 ka BP (Alder & Hostetler, 2014), large *Picea* populations have been restricted to elevations between 2,400 and 2,700 m.
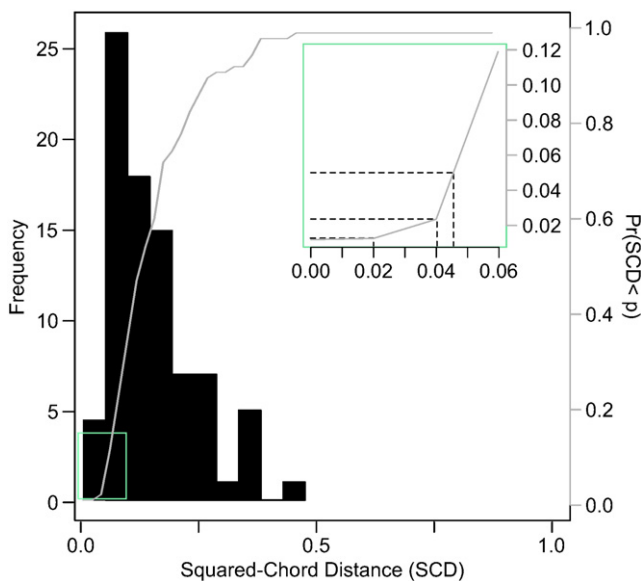

FIGURE 3 Relative frequency of square-chord distances (SCDs) between all pairs of pollen samples considered in this study (in black), and probability of theoretical SCD values (as estimated with a Monte Carlo simulation (1,000 runs)) of being smaller than the calculated SCDs (Pr(SCD)<p; in gray). The inset shows an enlargement of the area delimited in green. The dashed lines depict critical thresholds of dissimilarity among vegetation zones at different significance levels (i.e. SCDs = .02, .04 and .046; $p = .01$, .025 and .05 respectively) [Colour figure can be viewed at wileyonlinelibrary.com]

The spatial-temporal patterns of *Abies* were similar to those of *Picea* in that it was present between 1,800 and 2,400 m elev prior to 15 ka BP and expanded to higher elevations at *c.* 13 ka BP (Figure 4). From 9 to 7 ka BP, large populations colonized elevations up to 3,000 m, but after 7.5 ka BP, *Abies* was abundant only between 2,400 and 2,700 m elev ($p > .80$; Table 1). *Abies* macrofossils were not recovered at any of the sites.

Large *Pinus* subgenus *Strobus* pollen percentages at 16 ka BP suggest that *Pinus albicaulis* and/or *P. flexilis* also established at low and middle elevations soon after ice recession ($p > .82$; Table 1; Figure 4). Populations were initially large between 1,850 and 2,400 m elev, but by 12.5 ka BP, one or both of these species was abundant at all elevations. Needles assigned to *P. albicaulis* at Mariposa Lake and Buckbean Fen attest to the local presence of the taxon above 2,360 m elev at this time (Whitlock, 1993). This extended distribution persisted until 7.5 ka BP and is attributed to warmer summers and more fires during the early Holocene (Alder & Hostetler, 2014; Figure 5a,b). Pollen isolines suggest a bimodal distribution in *P.* subgenus *Strobus* in the last 4,000 years that likely represents the dominance of *P. albicaulis* at high elevations and *P. flexilis* at low elevations.

Pinus subgenus *Pinus* and Total *Pinus* pollen percentages increased after 11 ka BP, indicating that *P. contorta* colonized its complete modern distribution at this time ($p > 0.75$; Table 1; Figure 4). This interpretation is confirmed by the presence of *P. contorta* needles at Hedrick Pond, Fallback Lake, Buckbean Fen and Cygnet Lake (Whitlock, 1993). Fast regeneration after disturbance apparently offered a competitive advantage to *P. contorta* over other conifers (Baker, 2009), especially in the early Holocene when regional fire activity was higher (Figure 5). *P. contorta* has been most abundant in the last 9,000 years at middle elevations (2,000–2,600 m elev), in part because of its ability to outcompete other conifers on the infertile rhyolite soils of central Yellowstone (Despain, 1990; Whitlock, 1993).

Pseudotsuga menziesii was rare to absent over much of the GYE prior to 12 ka BP ($p > .87$; Table 1; Figure 4) and fluctuated in abundance at middle and low elevations between 12 and 8 ka BP. Plant macrofossils of *Pseudotsuga* at Fallback Lake and Buckbean Fen suggest that it grew at higher elevations in the early Holocene than at present. *Pseudotsuga* was present below 2,000 m elev after 8 ka BP ($p > .80$; Table 1), although its abundance varied through time. The species reached greatest abundance during the Medieval Climate Anomaly (1.2–0.8 ka BP; Meyer, Wells, & Jull, 1995) when dry conditions and frequent low-severity fires promoted its dominance (Millspaugh et al., 2004).

In summary, conifers began to colonize newly deglaciated landscapes after 16 ka BP, starting at low and middle elevations and reaching higher landscapes by 12 ka BP. The sequence of conifer expansion matches species' current tolerances to temperature and moisture stress (i.e. from cold-tolerant subalpine taxa (*Picea spp*, *Abies lasiocarpa*, *Pinus albicaulis* and/or *P. flexilis*) to drought-tolerant *Pinus contorta* and *Pseudotsuga*; Figure 4). Upslope expansion in the late-glacial to early-Holocene transition was likely governed by rising temperatures and decreased moisture availability in association with increased summer insolation (Alder & Hostetler, 2014). Differences
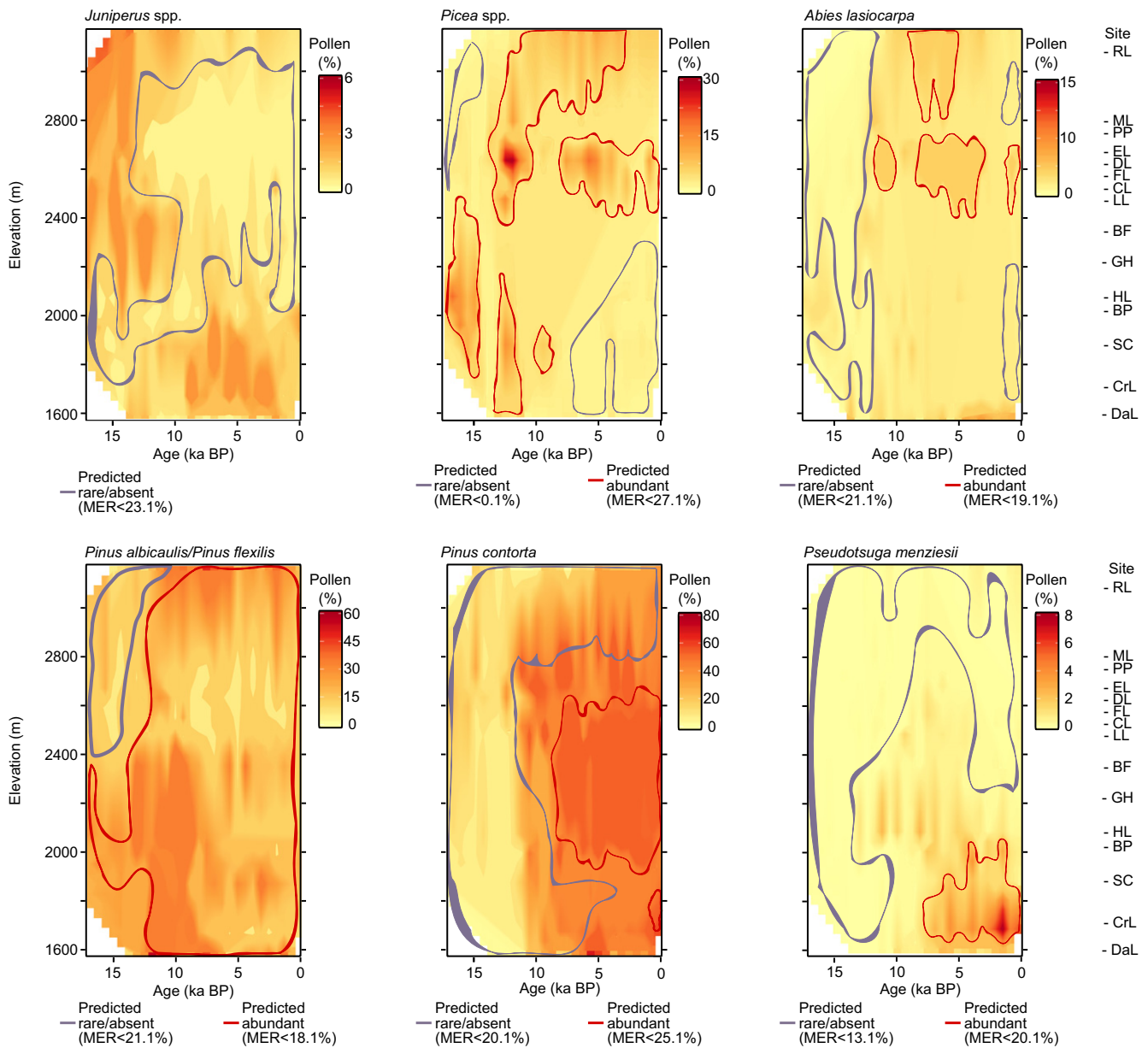
FIGURE 4 Pollen isolines (i.e. lines of equal pollen abundance) based on bivariate interpolation of pollen percentages onto a grid defined by elevation and time. The red (gray) lines show the locations and times when the classification trees predict each taxon to be abundant (absent/rare). Misclassification error rates (MERs) for each taxon are also given. The elevation of the sites employed in the analysis is indicated (RL: Rapid Lake; ML: Mariposa Lake; PP: Park Pond; EL: Emerald Lake; DL: Divide Lake; FL: Fallback Lake; CL: Cygnet Lake; LL: Lily Lake; BF: Buckbean Fen; GH: Gardiner's Hole; BP: Blacktail Pond; SC: Slough Creek; CrL, Crevice Lake; DaL: Dailey Lake; Table S1 in Appendix S2) [Colour figure can be viewed at wileyonlinelibrary.com]
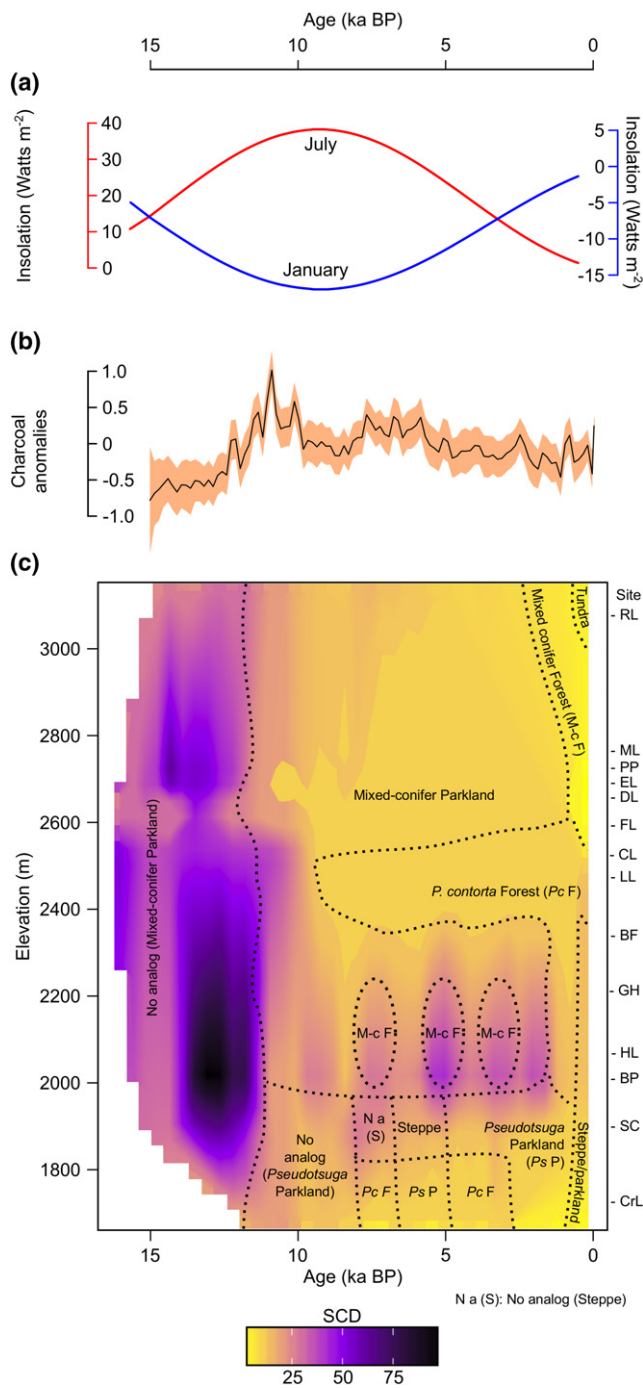
in the spatial and temporal patterns of genera with similar climate tolerances (e.g. *Picea* and *Abies*) as well as the dominance of *P. contorta* in central Yellowstone region attest to the role of disturbance, soil fertility and competition in shaping vegetation at the local scale (Iglesias et al., 2015; Krause & Whitlock, 2017).

4.2 | Environmental history of the GYE

The vegetation reconstruction draws on (a) optimal thresholds of dissimilarity based on SCDs employed to identify the closest modern analogue for each fossil assemblage; (b) cover classes (i.e. Open,

Parkland and Forest Cover) derived from the sequentially partitioning of the modern pollen dataset; and (c) SCDs between fossil pollen samples and the youngest sample of each record, which are interpreted as a proxy of the local vegetation trajectory. The pollen-based vegetation reconstruction is compared with a published composite of six charcoal records from different elevations in the GYE (Iglesias et al., 2015) and July and January insolation anomalies to provide insights on past ecological changes in light of large-scale changes in climate (Figure 5).

Space-for-time substitutions indicate that extensive open parkland with *Artemisia* and *Juniperus* dominated the GYE soon after ice

FIGURE 5 Environmental history in the GYE over the last 16,000 years. (a) January (blue) and July (red) insolation anomalies with respect to present-day at latitude 45°N (Berger & Loutre, 1991). (b) Trends in regional fire activity as reconstructed from anomalies in charcoal data from six sites (Iglesias et al., 2015). The orange shading represents 95% confidence intervals. (c) Vegetation trajectory at each site as inferred from interpolated squared-chord distances (SCD) between each fossil pollen sample and the youngest sample of a particular record. High SCD values (purple) are most different from the present-day pollen sample at each site, and low SCD values (yellow) are a close match to the present-day sample. The dashed lines mark abrupt changes in vegetation identified through sequential Lepage testing of SCD values. Reconstructed vegetation is based on optimal thresholds of dissimilarity (p < 0.05). Samples were assigned to the No-analogue vegetation class (N a) when the SCD between them and the modern pollen assemblages from all vegetation zones exceeded the optimal threshold of dissimilarity. In those cases, the most similar analogue is indicated. The elevation of the sites employed in the analyses is shown (RL: Rapid Lake; ML: Mariposa Lake; PP: Park Pond; EL: Emerald Lake; DL: Divide Lake; FL: Fallback Lake; CL: Cygnet Lake; LL: Lily Lake; BF: Buckbean Fen; GH: Gardiner's Hole; BP: Blacktail Pond; SC: Slough Creek; CrL, Crevice Lake; Table S1 in Appendix S2) [Colour figure can be viewed at wileyonlinelibrary.com]

the vegetation change at 12 ka BP at all elevations suggests that an ecological threshold was crossed in response to these gradual climate changes.

The amplification of the seasonal cycle of insolation between 12 and 6 ka BP was correlated with rising temperatures, relative high winter precipitation and effectively dry conditions (Figure 5a; Alder & Hostetler, 2014). Conversely, the last 6,000 years featured cooler, wetter summers and warmer, drier winters in this region (Whitlock et al., 2012). Charcoal data suggest steadily rising regional fire activity following deglaciation, possibly as a function of higher temperatures and increasing fuel biomass. Maximum fire values were reached between 12 and 9 ka BP during the July insolation maximum. Fire activity decreased between 9 and 7.5 ka BP, increased slightly from 7 to 5 ka and then declined more steadily after 5 ka BP, matching the onset of cooler wetter conditions in the GYE.

Sites above 2,600 m elev featured Mixed-conifer Parkland from 12 to 1.5 ka BP. The relative dominance of species, nonetheless, changed through this period (Figure 4) and the fire history was very dynamic (Figure 5b). At 1.5 ka BP, parkland was replaced by Mixed-conifer Forest, possibly in response to higher temperatures during the Medieval Climate Anomaly. Tundra expansion at the highest elevations at 0.5 ka BP (Rapid Lake, 3,134 m elev) led to lowering of upper tree line, which is attributed to Little Ice Age cooling (1500–1890 AD).

Between 2,400 and 2,600 m elev, the Mixed-conifer association that formed at 12 ka BP was short-lived. At Fallback Lake (2,572 m elev), Cygnet Lake (2,531 m elev) and Lily Lake (2,458 m elev), Mixed-conifer Parkland was replaced by Pinus contorta Forest at 9 ka BP, when summer insolation and regional fire activity reached their maximum Holocene values (Figure 5). This forest has persisted at middle elevations to the present day, in part as a result of edaphic effects as well as by frequent fires (Baker, 2009).

recession. The high level of dissimilarity between fossil and modern pollen assemblages between 16 and 12 ka BP suggests that the arrival of Picea, Abies and Pinus (Figure 4) formed a series of transient vegetation types with no modern counterpart in the GYE vegetation (p < .05). The emergence of the Picea, Abies, Pinus albicaulis/P. flexilis association occurred abruptly at c. 12 ka BP when Mixed-conifer Parkland became widespread at elevations above 2,000 m. The initial sequence of postglacial vegetation development was associated with rising summer insolation (Figure 5a) and a northward shift of the jet stream from its full-glacial position, bringing warmer and wetter conditions to the region (Alder & Hostetler, 2014). The abruptness of

At middle elevations (2,000–2,400 m), a mixed-conifer association also was present from 12 to 1.5 ka BP, but variability in tree pollen abundance during this period suggests centennial-scale fluctuations between forest and parkland. At 1.5 ka, *P. contorta* Forest expanded downslope and replaced Mixed-conifer Forest/Parkland as the dominant vegetation. This abrupt vegetation change was associated with, and possibly favoured by, a shift from high-frequency surface fires to low-frequency, high-severity fires (Huerta et al., 2009). Charcoal data from Blacktail Pond (2,012 m elev) suggest that periods of Mixed-conifer Forest co-occurred with infrequent, severe fires (e.g. 11–8.5 and 7.6–6 ka BP) while times of parkland supported frequent, small fires (e.g. 8.5–7.6 ka BP).

At low elevations (<2,000 m elev), parkland of *Artemisia*, *Pinus*, *Juniperus* and scattered *Pseudotsuga* developed between 12 and 8 ka BP. This community has no exact analogue in the modern GYE, given the low representation of *Pseudotsuga*-type in the fossil pollen assemblages (Figure 5c). From 8 to 2.5 ka, the vegetation mosaic varied across the region ranging between no-analogue *Artemisia*-dominated steppe, *Pseudotsuga* Parkland and *Pinus contorta* Forest. During the last 500 years, Steppe/parkland has dominated all the low-elevation sites, indicating upslope migration of lower tree line (Figure 5c). This contraction was probably driven by decreased moisture availability (Whitlock et al., 2012) and higher fire activity (Figure 5a,c).

Both stability and rapid change are noted in the regional vegetation history. Two particular examples of persistent plant communities suggest a long-term resilience to climate change. First, mixed conifer associations, with *Picea*, *Abies* and *Pinus*, have dominated the high and middle elevations for the last 12,000 years ($p > .81$; Table 1). While the association has been relatively stable in terms of composition and distribution, changes in tree density, especially at low and middle elevations, have led to periods of forest and parkland. These variations were likely related to centennial-scale variations in climate and disturbance (Whitlock et al., 2012). Second, *Pinus contorta* Forest has occupied elevations from 2,400 to 2,600 m through the last 9,000 years with little change in composition despite changes in effective moisture and disturbance (Millspaugh et al., 2000). Stability in this case is conferred by edaphic constraints that limit the competitive success of other conifers (Despain, 1990).

In contrast, low-elevation vegetation has been highly heterogeneous and temporally variable during the last 8,000 years. Shifts between forest, parkland and steppe below 2,000 m elev are attributed to variations in effective moisture and fire as inferred from oxygen isotope, diatom and charcoal data from Crevice Lake (Whitlock et al., 2012). In the last *c.* 1,000–500 years, the low elevations have been the most open, presumably as a legacy of increased drought during and following the Medieval Climate Anomaly. In contrast, high-elevation forests have responded to cooling during the Little Ice Age by shifting upper tree line downslope. As a consequence of a temperature-driven lowering of upper tree line and a moisture-triggered upslope expansion of steppe in recent centuries, the modern elevational distribution of forest in the GYE is now more limited than at any time in the last 12,000 years.

5 | CONCLUSIONS

The dual examination of modern and fossil pollen data provides a more robust basis for reconstructing long-term vegetation dynamics in the GYE, and particularly for assessing ecosystem response to past environmental change. The history of species and vegetation types offers insights about the vulnerability of the GYE and other mountain ecosystems to future climate change. In particular, our results suggest the following:

(i) Most of the conifers have been present in the GYE for at least the last 12,000 years and survived past climate change by adjusting their elevational ranges. Site-specific abundance, nonetheless, has been affected by local disturbance, competition and edaphic conditions. This dependence on both large-scale elevation gradients and watershed-scale constraints highlights the importance of large protected areas in maximizing the ability of species to adapt to future climate change.

(ii) Mixed-conifer forest and parkland of *Picea*, *Abies* and *Pinus* have exhibited exceptional stability over millennia by adjusting their elevational range. The current mixed-conifer distribution, however, is more restricted than at any time in its history, and the association is highly vulnerable to projected warming in the future (Chang, Hansen, Piekieleck, Chang, & Phillips, 2014).

(iii) *Pinus contorta* forest has been present for about 9,000 years and will probably persist in the future, given its ability to tolerate warm temperatures, fire, infertile soils and competing conifers.

(iv) Below 2,000 m elev, transient, and sometimes novel associations of forest, parkland and steppe have occurred on submillennial time scales. Similar dynamic responses seem likely in the future especially at lower tree line, where *Pseudotsuga* parkland is vulnerable to drought and severe fires.

(v) Present-day forest cover is elevationally compressed compared with previous millennia probably due to the legacy of the Medieval Climate Anomaly and the Little Ice Age. The recent upslope rise in lower tree line suggests a heightened role for fire and drought at low elevations, whereas the downslope lowering of upper tree line and forest marks cooler conditions at high elevations in recent centuries. The current vegetation distribution is, at best, a short and rather anomalous baseline for evaluating ecological responses to future climate change.

(vi) Incorporating palaeoecological data into vulnerability assessments lengthens the baseline of observation and provides information over a broader range of conditions than has occurred in recent decades (Whitlock, Colombaroli, Conedera, & Tinner, 2018). The ability to assign levels of certainty to the reconstruction, as was done in this study, is an important step in the use of these data for assessing an ecosystem's capacity to withstand environmental change in the future.

DATA ACCESSIBILITY

ORCID

Virginia Iglesias (iD) http://orcid.org/0000-0001-5732-3714

REFERENCES

Adler, D. (2005). *vioplot: Violin plot. R package version 0.2*. Retrieved from http://wsopuppenkiste.wiso.uni-goettingen.de/~dadler

Akima, H. (1978). A method of bivariate interpolation and smooth surface fitting for irregularly distributed data points. *ACM Transactions of Mathematical Software*, *4*, 148e159.

Akima, H., & Gebhardt, A. (2016). *akima: Interpolation of irregularly and regularly spaced data. R package version 0.6-2*. Retrieved from https://CRAN.R-project.org/package=akima

Alder, J., & Hostetler, S. W. (2014). Global climate simulations at 3000 year intervals for the last 21,000 years with the GENMOM coupled atmosphere-ocean model. *Climate of the Past*, *10*, 2925–2978. https://doi.org/10.5194/cpd-10-2925-2014

Baker, R. G. (1976). Late Quaternary vegetation history of the Yellowstone Lake Basin, Wyoming. United States Geological Survey Professional Paper: 729-E.

Baker, W. L. (2009). *Fire ecology in Rocky Mountain landscapes* (p. 605). Washington, DC: Island Press.

Baker, R. G., & Richmond, G. M. (1978). Geology, palynology, and climatic significance of two pre-Pinedale lake sediment sequences in and near Yellowstone National Park. *Quaternary Research*, *10*, 226–240. https://doi.org/10.1016/0033-5894(78)90103-5

Berger, A., & Loutre, M. (1991). Insolation values for the climate of the last 10 million years. *Quaternary Science Reviews*, *10*, 297–317. https://doi.org/10.1016/0277-3791(91)90033-Q

Breiman, L., Friedman, J., Stone, C. J., & Olshen, R. A. (1984). *Classification and regression trees* (p. 359). Belmont, CA: Wadsworth.

Brunelle, A., Whitlock, C., Bartlein, P. J., & Kipfmuller, K. (2005). Postglacial fire, climate, and vegetation history along an environmental gradient in the Northern Rocky Mountains. *Quaternary Science Reviews*, *24*, 2281–2300. https://doi.org/10.1016/j.quascirev.2004.11.010

Cañellas-Boltà, N., Rull, V., Vigo, J., & Mercadé, A. (2009). Modern pollen-vegetation relationships along an altitudinal transect in the central Pyrenees (southwestern Europe). *The Holocene*, *19*, 1185–1200. https://doi.org/10.1177/0959683609345082

Chang, T., Hansen, A. J., Piekieleck, N., Chang, T., & Phillips, L. B. (2014). Patterns and variability of projected bioclimatic habitat for *Pinus albicaulis* in the Greater Yellowstone Area. *PLoS ONE*, *9*(11), e111669. https://doi.org/10.1371/journal.pone.0111669

Despain, D. G. (1990). *Yellowstone vegetation: Consequences of environment and history in a natural setting*. Boulder, CO: Roberts Rinehart, p. 239.

Haselhorst, M. S. H., & Buerkle, C. A. (2013). Population genetic structure of *Picea engelmannii*, *P. glauca* and their previously unrecognized hybrids in the central Rocky Mountains. *Tree Genetics and Genomes*, *9*, 669–681. https://doi.org/10.1007/s11295-012-0583-7

Huerta, M. A., Whitlock, C., & Yale, J. (2009). Holocene vegetation–fire–climate linkages in northern Yellowstone National Park, USA. *Palaeogeography, Palaeoclimatology, Palaeoecology*, *271*, 170–181. https://doi.org/10.1016/j.palaeo.2008.10.015

Iglesias, V., Krause, T., & Whitlock, C. (2015). Complex response of *Pinus albicaulis* to past environmental variability increases understanding of its future vulnerability. *PLoS ONE*, *10*(4), e0124439. https://doi.org/10.1371/journal.pone.0124439

Iglesias, V., Quintana, F., Nanavati, W., & Whitlock, C. (2016). Interpreting modern and fossil pollen data along a steep environmental gradient in northern Patagonia. *The Holocene*, *27*, 1008–1018.

Juggins, S. (2017). *rioja: Analysis of Quaternary science data. R package version 0.9-15*. Retrieved from http://cran.r-project.org/package=rioja

Krause, T. R., Lu, T., Whitlock, C., Fritz, S., & Pierce, K. L. (2015). Patterns of terrestrial and limnologic development during the late-glacial/early-Holocene transition inferred from multiple proxy records from Dailey Lake, Montana, USA. *Palaeogeography, Palaeoclimatology, Palaeoecology*, *422*, 46–56. https://doi.org/10.1016/j.palaeo.2014.12.018

Krause, T. R., & Whitlock, C. (2013). Climate and vegetation change during the late-glacial/early-Holocene transition inferred from multiple proxy records from Blacktail Pond, Yellowstone National Park, USA. *Quaternary Research*, *79*, 391–402. https://doi.org/10.1016/j.yqres.2013.01.005

Krause, T. R., & Whitlock, C. (2017). Climatic and non-climatic controls shaping early postglacial conifer history in the northern Greater Yellowstone Ecosystem, USA. *Journal of Quaternary Science*, *32*, 1022–1036. https://doi.org/10.1002/jqs.2973 https://doi.org/10.1002/jqs.2973

Licciardi, J. M., & Pierce, K. L. (2008). Cosmogenic exposure-age chronologies of Pinedale and Bull Lake glaciations in Greater Yellowstone and the Teton range, USA. *Quaternary Science Reviews*, *27*, 814e831.

Markgraf, V., Webb, R. S., Anderson, K., & Anderson, L. (2002). Modern pollen/climate calibration for southern South America. *Palaeogeography, Palaeoclimatology, Palaeoecology*, *181*, 375–397. https://doi.org/10.1016/S0031-0182(01)00414-X

Meyer, G. A., Wells, S. G., & Jull, A. J. T. (1995). Fire and alluvial chronology in Yellowstone National Park: Climatic and intrinsic controls on Holocene geomorphic processes. *Geological Society of America Bulletin*, *107*, 1211–1230. https://doi.org/10.1130/0016-7606(1995)107<1211:FAACIY>2.3.CO;2

Millspaugh, S. H., Whitlock, C., & Bartlein, P. J. (2000). Variations in fire frequency and climate over the past 17 000 yr in central Yellowstone National Park. *Geology*, *28*, 211–214. https://doi.org/10.1130/0091-7613(2000)28<211:VIFFAC>2.0.CO;2

Millspaugh, S. H., Whitlock, C., & Bartlein, P. J. (2004). Postglacial fire, vegetation, and climate history of the Yellowstone-Lamar and Central Plateau provinces, Yellowstone National Park. In L. Wallace (Ed.), *After the fires: The ecology of change in Yellowstone National Park* (pp. 10–28). New Haven, CT: Yale University Press. https://doi.org/10.12987/yale/9780300100488.001.0001

Minckley, T., & Whitlock, C. (2000). Spatial variation of modern pollen in Oregon and southern Washington, USA. *Review of Palaeobotany and Palynology*, *112*, 97–123. https://doi.org/10.1016/S0034-6667(00)00037-3

Mumma, S. A., Whitlock, C., & Pierce, K. P. (2012). A 28,000-year history of vegetation and climate from Lower Red Rock Lake, Centennial Valley, southwestern Montana, USA. *Palaeogeography, Palaeoclimatology, Palaeoecology*, *326–328*, 30–41.

Overpeck, J. T., Webb, T. III, & Prentice, I. C. (1985). Quantitative interpretation of fossil pollen spectra: Dissimilarity coefficients and the method of modern analogs. *Quaternary Research*, *23*, 87–108. https://doi.org/10.1016/0033-5894(85)90074-2

R Core Team (2016). *R: A language and environment for statistical computing*. Vienna, Austria: R Foundation for Statistical Computing. Retrieved from https://www.R-project.org/

Ripley, B. D. (1996). *Pattern recognition and neural networks* (p. 403). Cambridge: Cambridge University Press. https://doi.org/10.1017/CBO9780511812651

Ripley, B. D. (2016). *tree: Classification and regression trees. R package version 1.0-37*. Retrieved from https://CRAN.R-project.org/package=tree

Sanders, H. L. (1968). Marine benthic diversity: A comparative study. *The American Naturalist*, *102*, 243–282. https://doi.org/10.1086/282541

Sawada, M. (2012). *MATTOOLS: Modern calibration functions for the Modern Analog Technique (MAT)*. R package version 1.1. Retrieved from https://CRAN.R-project.org/package=MATTOOLS

Sawada, M., Viau, A. E., Vettoretti, G., Peltier, W. R., & Gajewski, K. (2004). Comparison of North-American pollen-based temperature and global lake-status with CCCma AGCM2 Output at 6 ka. *Quaternary Science Reviews*, *23*, 225–244. https://doi.org/10.1016/j.quascirev.2003.08.005

Thompson, R. S., Anderson, K. H., & Bartlein, P. J. (1999). *Atlas of relations between climatic parameters and distributions of important trees and shrubs in North America*. U.S. Geological Survey Professional Paper 1650

Waddington, J. C., & Wright, H. E. Jr (1974). Late Quaternary vegetational changes on the east side of Yellowstone National Park, Wyoming. *Quaternary Research*, *4*, 175–184.

Whitlock, C. (1993). Postglacial vegetation and climate of Grand Teton and southern Yellowstone national parks. *Ecological Monographs*, *63*, 173–198. https://doi.org/10.2307/2937179

Whitlock, C., & Bartlein, P. J. (1993). Spatial variations of Holocene climatic change in the Yellowstone region. *Quaternary Research*, *39*, 231–238. https://doi.org/10.1006/qres.1993.1026

Whitlock, C., Colombaroli, D., Conedera, M., & Tinner, W. (2018). Land-use history as a guide for forest conservation and management. *Conservation Biology*, *32*, 84–97. https://doi.org/10.1111/cobi.12960

Whitlock, C., Dean, W. E., Fritz, S. C., Stevens, L. R., Stone, J. R., Power, M. J., … Bracht-Flyr, B. B. (2012). Holocene seasonal variability inferred from multiple proxy records from Crevice Lake, Yellowstone National Park, USA. *Palaeogeography, Palaeoclimatology, Palaeoecology*, *331*, 90–103. https://doi.org/10.1016/j.palaeo.2012.03.001

Whitlock, C., & Larsen, C. P. S. (2001). Charcoal as a fire proxy. In J. P. Smol, H. J. B. Birks, & W. M. Last (Eds.), *Tracking environmental change using lake sediments*, Vol. *3* (pp. 75–97)., *Terrestrial, Algal, and Siliceous Indicators* Dordrecht, the Netherlands: Kluwer Academic Publishers.

Wickham, H. (2016). *ggplot2: Elegant graphics for data analysis*. New York, NY: Springer-Verlag. https://doi.org/10.1007/978-3-319-24277-4

Williams, J. W., & Jackson, S. T. (2007). Novel climates, non-analog communities, and ecological surprises. *Frontiers in Ecology and the Environment*, *5*, 475–482. https://doi.org/10.1890/070037

BIOSKETCH

The authors are palaeoecologists with extensive experience in reconstructing long-term linkages between climate, vegetation and fire in the temperate forests of the Northern and Southern Hemispheres. The study is part of a collaborative effort to understand the causes and consequences of climate change in the past, present and future.

Author contributions: V.I. and C.W. conceived the ideas; C.W., T.R.K. and R.G.B. collected the data; V.I. analysed the data and V.I. and C.W. led the writing.

SUPPORTING INFORMATION

Additional supporting information may be found online in the Supporting Information section at the end of the article.